



# An analytical solution for the free vibration of FG nanoplates

Lazreg Hadji<sup>1,2</sup> · Mehmet Avcar<sup>3</sup> · Ömer Civalek<sup>4</sup>

Received: 25 February 2021 / Accepted: 30 July 2021 / Published online: 17 August 2021  
© The Brazilian Society of Mechanical Sciences and Engineering 2021

## Abstract

In the present work, an analytical solution for the free vibration of nanoplates made of functionally graded materials (FGMs) under various boundary conditions is provided. In this context, a new refined plate theory with four variables based on the theory of non-local elasticity including the small-scale influences is adopted. Using the rule of mixture, the material properties of nanoplates are supposed to vary continuously across the thickness direction. Based on Eringen's non-local elasticity theory, the equations of motion of functionally graded (FG) nanoplate are derived using Hamilton's principle, and the obtained equations are solved analytically. Here, the number of unknowns and governing equations of the present model are reduced to four separating the vertical displacement into shear and bending components, and so the number of unknowns has become less than the other alternative theories. The influences of the different parameters such as vibration mode, the aspect ratio, boundary conditions, power-law index, and non-local parameter on the natural frequencies of the FG nanoplate are discussed, in detail. Finally, it is decided that the considered parameters have major influence on the natural frequencies of the FG nanoplates. Furthermore, the proposed solution method not only satisfactorily handled the present problem and yielded successful results but also it supplied ease in the examination of non-local free vibration of FG nanoplates.

**Keywords** Free vibration · Analytical solution · Non-local theory · FGMs · Nanoplate

## 1 Introduction

The new kind of composites with smoothly varying material properties changing the volume fraction of constituents gradually along with one or more directions is called FGMs. In comparison with the traditional composite materials, FGMs exhibit not only superior features such as extremely high stiffness and strength combined with a very low density, resistance to chemicals, thermal and electrical insulation but also eliminate stress concentrations at the interfaces of composites [1, 2]. FGMs are regularly composed of two different

kinds of structural components like ceramic and metal, and the volume fractions of these constituents change as a function of the certain dimensions of the structure to realize the desired functions. FGMs have a wide application range in modern technology including aerospace, medicine, defense, energy, optoelectronics, automotive, biotechnology, aviation, civil, and mechanical engineering [3–10].

Since the introduction of carbon nanotubes (CNTs) by Iijima [11], nanotechnology has become an important part of mankind as a result of the rapidly increasing use of nanosized structures in modern life as well as in defense technology for the miniaturization of information technology devices. Nanowires, nanotubes, nanobeams, nanomembranes, and nanoplates are some examples of nano-sized structures composed of nanomaterials with outstanding mechanical, chemical, electronic, electrical, and optical properties, and they have utilization in nano-/microelectromechanical systems (NEMS/MEMS), aerospace, biomedical and bioelectrical devices; some examples are photovoltaic cell, generators, micro-/nano-switches resonators, sensors, energy harvesting, transistors, and atomic force microscopy [12–21].

---

Technical Editor: Monica Carvalho.

✉ Mehmet Avcar  
mehmetavcar@yahoo.com; mehmetavcar@sdu.edu.tr

<sup>1</sup> Laboratory of Geomatics and Sustainable Development, University of Tiaret, Tiaret, Algeria

<sup>2</sup> Department of Mechanical Engineering, University of Tiaret, BP 78 Zaaroura, 14000 Tiaret, Algeria

<sup>3</sup> Department of Civil Engineering, Faculty of Engineering, Suleyman Demirel University, Cunur, Isparta, Turkey

<sup>4</sup> China Medical University, Taichung, Taiwan

Nanostructures have ridiculously small dimensions that are comparable to the size of their material microstructure, and therefore, it becomes essential to study the size effect as the mechanical behaviors of nanostructures. Several approaches have been developed to capture the size influences as experimental, molecular dynamics simulations, and continuum mechanics. However, continuum mechanics is the most widely used method between these approaches because it is easy, cost-efficient, and effective. But the classical continuum mechanics cannot capture the size influence since the constitutive model of it does not include the material length parameters. Thus, a variety of size-dependent continuum mechanics approaches are established such as the surface elasticity theory, non-local elasticity theory, the modified couple stress theory, and strain gradient elasticity theory. Between these approaches, Eringen's non-local elasticity theory contains only one scale parameter of small length for the definitions of the internal length scale of nanostructures and atomic forces, and hence, it has been widely employed [22–24].

Currently, the investigations on the mechanical behaviors of nanoplates composed of FGMs have attracted many researchers due to the increasing demand for applications of these structures in modern technology because of their superior properties. In various engineering practices, structural elements are exposed to dynamic loads, which can excite the structural vibrations and induce durability concerns or discomfort due to the resulting noise and vibration. Besides, if the vibration exceeds particular limits, breakage or failure may occur. Since FG nanoplates have been started to be used in micro-/nanoelectromechanical systems, such as the components in the form of shape-memory alloy thin films with a global thickness in micro- or nano-scale [25, 26], electrically actuated MEMS devices [27, 28], and atomic force microscopes [29], as well as medicines, gas sensors, energy storage, field emission, transportation of nano-cars and solar cells [30–32], the vibration analysis of nanoplates has been a vital task in their design for engineers and researchers for recent years. Gürses et al. [33] performed numerical computations using discrete singular convolution for the free vibration of nano-annular sector plates based on non-local continuum theory. The size-dependent free vibration of FG nanoplates is examined by Natarajan et al. [34] using the isogeometric-based finite element method. The three-dimensional non-local bending and vibration analyses of FG nanoplates are performed by Ansari et al. [35] using the variational differential quadrature method. Daneshmehr et al. [36] studied the free vibration of FG nanoplate using the generalized differential quadrature method. Nami and Janghorban [37] presented the free vibration of rectangular nanoplates with simply supported boundary conditions depending on refined plate theory with two variables employing strain gradient elasticity theory. Mechab et al. [38] examined the

free vibration of FG nanoplate resting on Winkler–Pasternak elastic foundations based on refined plate theories with two variables including the effect of porosities. Phung-Van et al. [39] presented the size-dependent geometrically nonlinear transient analysis of FG nanoplates employing a solution procedure depending on isogeometric analysis combined with higher-order shear deformation theory. Arefi et al. [40] analyzed the free vibration of FG polymer composite nanoplates reinforced with graphene nanoplatelets resting on a Pasternak foundation applying a two-variable sinusoidal shear deformation theory adopting the non-local elasticity theory. Barati and Shahverdi [41] dealt with the semi-analytical nonlinear thermal vibration analysis of FG nanoplates modeled by four-variable refined plate theory. Zargaripour et al. [42] examined the free vibration of FG nanoplate using the finite element method. Baretta et al. [43] studied the size-dependent elastostatic responses of axisymmetric annular nano-plates using a stress-driven non-local integral methodology of elasticity. Ruocco and Mallardo [44] considered the buckling and vibration of imperfect nanoplates via non-local Mindlin plate theory employing a coupling finite strip–finite element procedure. Sharifi et al. [45] dealt with the vibration of FG piezoelectric nanoplates based on the non-local strain gradient theory, analytically. Daikh et al. [46] analyzed the free vibration of rectangular FGM sandwich nanoplates with simply supported boundary conditions. Tran et al. [47] analyzed the bending and free vibration of FG nanoplates resting on elastic foundations utilizing a finite element model using four-unknown shear deformation theory integrated with the non-local theory. Zenkour et al. [48] examined the bending of simply supported FG nanoplate utilizing the non-local mixed variational formula. Liu et al. [49] studied the thermo-electro-mechanical free vibration of piezoelectric nanoplates based on the non-local theory and Kirchhoff theory. Malekzadeh and Shojaee [50] investigated the free vibration of nanoplates utilizing a refined plate theory joint with the non-local theory. Kiani [51] examined the features of in-plane and out-of-plane free vibrations of a conducting nanoplate subjected to the unidirectional in plane steady magnetic field utilizing different non-local shear deformable plate theories.

From the results of the search of open literature, it is observed that numerous studies are devoted to examine the mechanical behaviors of FG nanoplates. In most of these studies, numerical solution methods are employed, the number of studies based on the exact solution is quite limited, and in these studies, the exact solutions are developed for simple support boundary conditions, generally. Because the free vibration of the FG nanoplates has great importance in modern technology, it has become a necessity to derive a reliable exact solution for this behavior under different boundary conditions. Therefore, in the current study, an attempt is done to address this problem. For this aim, an

exact analytical solution for the free vibration of nanoplates made of FGMs under four different boundary conditions is provided. The influence of the different parameters such as vibration mode, the aspect ratio, boundary conditions, power-law index, and non-local parameter on the natural frequencies of the FG nanoplate is discussed, in detail.

## 2 The formulation of the problem

Figure 1 displays an FG nanoplate of length  $a$ , width  $b$ , and height  $h$ . It is supposed that the top surface of the nanoplate ( $z = +h/2$ ) is ceramic-rich and it is graded to the metal-rich one at the bottom surface ( $z = -h/2$ ).

The material properties,  $P$ , are supposed to grade across the thickness of FG nanoplate depending on the rule of the mixture as follows:

$$P(z) = P_c V_c + P_m V_m \tag{1}$$

where  $P_c$ ,  $P_m$ ,  $V_c$ , and  $V_m$  represent the material properties and volume fractions of the ceramic and metal constituents, respectively.

The total volume fraction of constituents is as follows:

$$V_m + V_c = 1 \tag{2}$$

The volume fraction of the ceramic constituent obeying the power-law distribution is as follows:

$$V_c = \left(\frac{z}{h} + \frac{1}{2}\right)^k \tag{3}$$

where  $k$  is a non-negative number and indicates the power-law index and  $z$  is the distance to the midplane of the nanoplate.

The efficient material properties of FG nanoplate could be expressed as:

$$E(z) = (E_c - E_m)V_c + E_m \tag{4a}$$

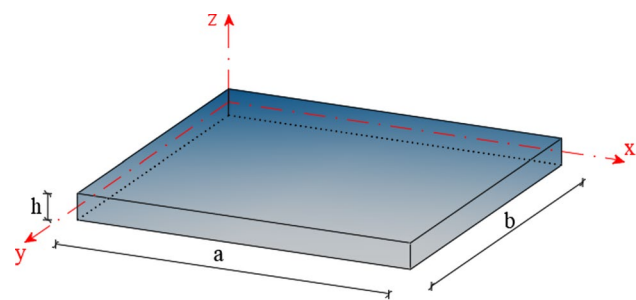


Fig. 1 The geometry of FG nanoplate

$$\rho(z) = (\rho_c - \rho_m)V_c + \rho_m \tag{4b}$$

where  $E$  and  $\rho$  are the Young’s modulus and the mass density of FG nanoplate, respectively.

Adopting Eringen’s [22, 23] non-local theory of elasticity, the influence of inter-atomic forces can be taken into account as the material parameters in the fundamental equation as follows:

$$(1 - \tau^2 L^2 \nabla^2) \sigma_{ij}^{NL} = \sigma_{ij}^L; \quad \tau^2 = \frac{\mu}{L^2} = \left(\frac{e_0 a}{L}\right)^2 \tag{5}$$

where superscripts (L, NL) denote the local and non-local, respectively,  $\mu = (e_0 a)^2$  is the non-local parameter representing the small-scale influence,  $e_0$  is a physical parameter that has been identified by experimental results, and  $a$  and  $L$  are the internal and external characteristic lengths, respectively.

Non-local constitutive equations of FG nanoplate are as follows:

$$\begin{Bmatrix} \sigma_x \\ \sigma_y \\ \tau_{xy} \\ \tau_{yz} \\ \tau_{xz} \end{Bmatrix} - \mu \left( \frac{\partial^2}{\partial x^2} + \frac{\partial^2}{\partial y^2} \right) \begin{Bmatrix} \sigma_x \\ \sigma_y \\ \tau_{xy} \\ \tau_{yz} \\ \tau_{xz} \end{Bmatrix} = \begin{bmatrix} Q_{11} & Q_{12} & 0 & 0 & 0 \\ Q_{12} & Q_{22} & 0 & 0 & 0 \\ 0 & 0 & Q_{44} & 0 & 0 \\ 0 & 0 & 0 & Q_{55} & 0 \\ 0 & 0 & 0 & 0 & Q_{66} \end{bmatrix} \begin{Bmatrix} \varepsilon_x \\ \varepsilon_y \\ \gamma_{yz} \\ \gamma_{xz} \\ \gamma_{xy} \end{Bmatrix} \tag{6}$$

where  $\sigma_x, \sigma_y, \tau_{xy}, \tau_{yz}, \tau_{xz}$  and  $\varepsilon_x, \varepsilon_y, \gamma_{xy}, \gamma_{yz}, \gamma_{xz}$  are the components of stress and strain, respectively, and  $C_{ij}$  are the stiffness coefficients and described as follows:

$$\begin{aligned} Q_{11} = Q_{22} &= \frac{E(z)}{1 - \nu^2}, & Q_{12} &= \frac{\nu E(z)}{1 - \nu^2}, \\ Q_{44} = Q_{55} = Q_{66} &= \frac{E(z)}{2(1 + \nu)} \end{aligned} \tag{7}$$

Note that the transverse normal stress is negligible in comparison with in-plane stresses in  $x$ - and  $y$ -axes.

The displacements of FG nanoplate depending on the higher-order shear deformable plate theory are [7, 52, 53]:

$$\begin{aligned} u(x, y, z, t) &= u_0(x, y, t) - z \frac{\partial w_b}{\partial x} - f(z) \frac{\partial w_s}{\partial x} \\ v(x, y, z, t) &= v_0(x, y, t) - z \frac{\partial w_b}{\partial y} - f(z) \frac{\partial w_s}{\partial y} \end{aligned} \tag{8}$$

$$w(x, y, z, t) = w_b(x, y, t) + w_s(x, y, t)$$

where  $u, v$ , and  $w$  denote the displacements throughout  $x, y$ , and  $z$  directions, respectively, and  $u_0, v_0, w_b$  and  $w_s$  are the unknowns as well as  $f(z)$  is the shape function and expressed as follows:

$$f(z) = z \left[ 1 + \frac{3\pi}{2} \operatorname{sech} \left( \frac{1}{2} \right)^2 \right] - \frac{3\pi}{2} h \tanh \left( \frac{z}{h} \right) \tag{9}$$

The nonzero strains related to the displacement field are:

$$\begin{Bmatrix} \epsilon_x \\ \epsilon_y \\ \gamma_{xy} \end{Bmatrix} = \begin{Bmatrix} \epsilon_x^0 \\ \epsilon_y^0 \\ \gamma_{xy}^0 \end{Bmatrix} + z \begin{Bmatrix} k_x^b \\ k_y^b \\ k_{xy}^b \end{Bmatrix} + f(z) \begin{Bmatrix} k_x^s \\ k_y^s \\ k_{xy}^s \end{Bmatrix} \tag{10}$$

$$\begin{Bmatrix} \gamma_{yz} \\ \gamma_{xz} \end{Bmatrix} = g(z) \begin{Bmatrix} \gamma_{yz}^s \\ \gamma_{xz}^s \end{Bmatrix}$$

where

$$\begin{Bmatrix} \epsilon_x^0 \\ \epsilon_y^0 \\ \gamma_{xy}^0 \end{Bmatrix} = \begin{Bmatrix} \frac{\partial u_0}{\partial x} \\ \frac{\partial v_0}{\partial y} \\ \frac{\partial u_0}{\partial y} + \frac{\partial v_0}{\partial x} \end{Bmatrix}, \quad \begin{Bmatrix} k_x^b \\ k_y^b \\ k_{xy}^b \end{Bmatrix} = \begin{Bmatrix} -\frac{\partial^2 w_b}{\partial x^2} \\ -\frac{\partial^2 w_b}{\partial y^2} \\ -2\frac{\partial^2 w_b}{\partial x \partial y} \end{Bmatrix}, \tag{11a}$$

$$\begin{Bmatrix} k_x^s \\ k_y^s \\ k_{xy}^s \end{Bmatrix} = \begin{Bmatrix} -\frac{\partial^2 w_s}{\partial x^2} \\ -\frac{\partial^2 w_s}{\partial y^2} \\ -2\frac{\partial^2 w_s}{\partial x \partial y} \end{Bmatrix}, \quad \begin{Bmatrix} \gamma_{yz}^s \\ \gamma_{xz}^s \end{Bmatrix} = g(z) \begin{Bmatrix} \frac{\partial w_s}{\partial y} \\ \frac{\partial w_s}{\partial x} \end{Bmatrix}$$

and then

$$g(z) = 1 - \frac{df(z)}{dz}$$

Utilizing Hamilton’s principle, the equations of motion could be found as follows:

$$0 = \int_0^t (\delta U - \delta K) dt \tag{12}$$

where  $\delta U$  and  $\delta K$  are the variations strain and kinetic energies, respectively.

The variation of strain energy of FG nanoplate can be specified as follows:

$$\begin{aligned} \delta U &= \int_V [\sigma_x \delta \epsilon_x + \sigma_y \delta \epsilon_y + \tau_{xy} \delta \gamma_{xy} + \tau_{yz} \delta \gamma_{yz} + \tau_{xz} \delta \gamma_{xz}] dV \\ &= \int_A \left[ N_x \delta \epsilon_x^0 + N_y \delta \epsilon_y^0 + N_{xy} \delta \gamma_{xy}^0 + M_x^b \delta k_x^b + M_y^b \delta k_y^b + M_{xy}^b \delta k_{xy}^b \right. \\ &\quad \left. + M_x^s \delta k_x^s + M_y^s \delta k_y^s + M_{xy}^s \delta k_{xy}^s + S_{yz}^s \delta \gamma_{yz}^s + S_{xz}^s \delta \gamma_{xz}^s \right] dA = 0 \end{aligned} \tag{13}$$

where  $A$  is the upper surface of FG nanoplate, and the stress resultants  $N$ ,  $M$ , and  $S$  can be described as follows:

$$(N_i, M_i^b, M_i^s) = \int_{-h/2}^{h/2} (1, z, f) \sigma_i dz, \quad (i = x, y, xy) \tag{14a}$$

$$(S_{xz}^s, S_{yz}^s) = \int_{-h/2}^{h/2} g(\tau_{xz}, \tau_{yz}) dz \tag{14b}$$

The variation of the kinetic energy of FG nanoplate can be specified as follows:

$$\begin{aligned} \delta T &= \int_{-h/2}^{h/2} \int_{\Omega} [\dot{u} \delta \dot{u} + \dot{v} \delta \dot{v} + \dot{w} \delta \dot{w}] \rho(z) d\Omega dz \\ &= \int_A \left\{ I_0 [\dot{u}_0 \delta \dot{u}_0 + \dot{v}_0 \delta \dot{v}_0 + (\dot{w}_b + \dot{w}_s)(\delta \dot{w}_b + \delta \dot{w}_s)] \right. \\ &\quad - I_1 \left( \dot{u}_0 \frac{\partial \delta \dot{w}_b}{\partial x} + \frac{\partial \dot{w}_b}{\partial x} \delta \dot{u}_0 + \dot{v}_0 \frac{\partial \delta \dot{w}_b}{\partial y} + \frac{\partial \dot{w}_b}{\partial y} \delta \dot{v}_0 \right) \\ &\quad - I_2 \left( \dot{u}_0 \frac{\partial \delta \dot{w}_s}{\partial x} + \frac{\partial \dot{w}_s}{\partial x} \delta \dot{u}_0 + \dot{v}_0 \frac{\partial \delta \dot{w}_s}{\partial y} + \frac{\partial \dot{w}_s}{\partial y} \delta \dot{v}_0 \right) \\ &\quad + J_1 \left( \frac{\partial \dot{w}_b}{\partial x} \frac{\partial \delta \dot{w}_b}{\partial x} + \frac{\partial \dot{w}_b}{\partial y} \frac{\partial \delta \dot{w}_b}{\partial y} \right) + K_2 \left( \frac{\partial \dot{w}_s}{\partial x} \frac{\partial \delta \dot{w}_s}{\partial x} + \frac{\partial \dot{w}_s}{\partial y} \frac{\partial \delta \dot{w}_s}{\partial y} \right) \\ &\quad \left. + J_2 \left( \frac{\partial \dot{w}_b}{\partial x} \frac{\partial \delta \dot{w}_s}{\partial x} + \frac{\partial \dot{w}_s}{\partial x} \frac{\partial \delta \dot{w}_b}{\partial x} + \frac{\partial \dot{w}_b}{\partial y} \frac{\partial \delta \dot{w}_s}{\partial y} + \frac{\partial \dot{w}_s}{\partial y} \frac{\partial \delta \dot{w}_b}{\partial y} \right) \right\} dA \end{aligned} \tag{15}$$

where the dot superscript demonstrates differentiation concerning the variable of time  $t$ ,  $I_i, J_i, K_i$  terms define the mass moment of inertias of FG nanoplate as follows:

$$(I_0, I_1, I_2) = \int_{-h/2}^{h/2} (1, z, z^2) \rho(z) dz \tag{16a}$$

$$(J_1, J_2, K_2) = \int_{-h/2}^{h/2} (f, z f, f^2) \rho(z) dz \tag{16b}$$

Inserting Eqs. (13) and (15) in Eq. (12) and after some mathematical operations and simplification, the subsequent equations are found

$$\begin{aligned} \delta u_0 &: \frac{\partial N_x}{\partial x} + \frac{\partial N_{xy}}{\partial y} = I_0 \ddot{u}_0 - I_1 \frac{\partial \ddot{w}_b}{\partial x} - J_1 \frac{\partial \ddot{w}_s}{\partial x} \\ \delta v_0 &: \frac{\partial N_{xy}}{\partial x} + \frac{\partial N_y}{\partial y} = I_{01} \ddot{v}_0 - I_1 \frac{\partial \ddot{w}_b}{\partial y} - J_1 \frac{\partial \ddot{w}_s}{\partial y} \\ \delta w_b &: \frac{\partial^2 M_x^b}{\partial x^2} + 2 \frac{\partial^2 M_{xy}^b}{\partial x \partial y} + \frac{\partial^2 M_y^b}{\partial y^2} \\ &= I_0 (\ddot{w}_b + \ddot{w}_s) + I_1 \left( \frac{\partial \ddot{u}_0}{\partial x} + \frac{\partial \ddot{v}_0}{\partial y} \right) - I_2 \nabla^2 \ddot{w}_b - J_2 \nabla^2 \ddot{w}_s \\ \delta w_s &: \frac{\partial^2 M_x^s}{\partial x^2} + 2 \frac{\partial^2 M_{xy}^s}{\partial x \partial y} + \frac{\partial^2 M_y^s}{\partial y^2} + \frac{\partial S_{xz}^s}{\partial x} + \frac{\partial S_{yz}^s}{\partial y} \\ &= I_0 (\ddot{w}_b + \ddot{w}_s) + J_1 \left( \frac{\partial \ddot{u}_0}{\partial x} + \frac{\partial \ddot{v}_0}{\partial y} \right) - J_2 \nabla^2 \ddot{w}_b - K_2 \nabla^2 \ddot{w}_s \end{aligned} \tag{17}$$

Inserting Eqs. (6) and (11) in Eq. (14) and after some mathematical operations, the stress resultants concerning generalized displacements ( $u_0, v_0, w_b, w_s$ ) are as follows:

$$\begin{aligned} \begin{Bmatrix} N \\ M^b \\ M^s \end{Bmatrix} - \mu \left( \frac{\partial^2}{\partial x^2} + \frac{\partial^2}{\partial y^2} \right) \begin{Bmatrix} N \\ M^b \\ M^s \end{Bmatrix} &= \begin{bmatrix} A & B & B^s \\ B & D & D^s \\ B^s & D^s & H^s \end{bmatrix} \begin{Bmatrix} \varepsilon \\ k^b \\ k^s \end{Bmatrix}, \\ S - \mu \left( \frac{\partial^2 S}{\partial x^2} + \frac{\partial^2 S}{\partial y^2} \right) &= A^s \gamma \end{aligned} \tag{18}$$

where

$$\begin{aligned} N &= \{N_x, N_y, N_{xy}\}^t, \quad M^b = \{M_x^b, M_y^b, M_{xy}^b\}^t, \\ M^s &= \{M_x^s, M_y^s, M_{xy}^s\}^t \end{aligned} \tag{19a}$$

$$\varepsilon = \{\varepsilon_x^0, \varepsilon_y^0, \gamma_{xy}^0\}^t, \quad k^b = \{k_x^b, k_y^b, k_{xy}^b\}^t, \quad k^s = \{k_x^s, k_y^s, k_{xy}^s\}^t \tag{19b}$$

$$A = \begin{bmatrix} A_{11} & A_{12} & 0 \\ A_{12} & A_{22} & 0 \\ 0 & 0 & A_{66} \end{bmatrix}, \quad B = \begin{bmatrix} B_{11} & B_{12} & 0 \\ B_{12} & B_{22} & 0 \\ 0 & 0 & B_{66} \end{bmatrix}, \quad D = \begin{bmatrix} D_{11} & D_{12} & 0 \\ D_{12} & D_{22} & 0 \\ 0 & 0 & D_{66} \end{bmatrix} \tag{19c}$$

$$\begin{aligned} B^s &= \begin{bmatrix} B_{11}^s & B_{12}^s & 0 \\ B_{12}^s & B_{22}^s & 0 \\ 0 & 0 & B_{66}^s \end{bmatrix}, \quad D^s = \begin{bmatrix} D_{11}^s & D_{12}^s & 0 \\ D_{12}^s & D_{22}^s & 0 \\ 0 & 0 & D_{66}^s \end{bmatrix}, \\ H^s &= \begin{bmatrix} H_{11}^s & H_{12}^s & 0 \\ H_{12}^s & H_{22}^s & 0 \\ 0 & 0 & H_{66}^s \end{bmatrix} \end{aligned} \tag{19d}$$

$$S = \{S_{xz}^s, S_{yz}^s\}^t, \quad \gamma = \{\gamma_{xz}^0, \gamma_{yz}^0\}^t, \quad A^s = \begin{bmatrix} A_{44}^s & 0 \\ 0 & A_{55}^s \end{bmatrix} \tag{19e}$$

where  $A_{ij}, B_{ij}, D_{ij}$  are the material stiffness coefficients and defined as follows:

$$\begin{aligned} &\begin{Bmatrix} A_{11} & B_{11} & D_{11} & B_{11}^s & D_{11}^s & H_{11}^s \\ A_{12} & B_{12} & D_{12} & B_{12}^s & D_{12}^s & H_{12}^s \\ A_{66} & B_{66} & D_{66} & B_{66}^s & D_{66}^s & H_{66}^s \end{Bmatrix} \\ &= \int_{-h/2}^{h/2} Q_{11}(1, z, z^2, f(z), zf(z), f^2(z)) \begin{Bmatrix} 1 \\ \nu \\ \frac{1-\nu}{2} \end{Bmatrix} dz \end{aligned} \tag{20a}$$

$$(A_{22}, B_{22}, D_{22}, B_{22}^s, D_{22}^s, H_{22}^s) = (A_{11}, B_{11}, D_{11}, B_{11}^s, D_{11}^s, H_{11}^s) \tag{20b}$$

$$A_{44}^s = A_{55}^s = \int_{-h/2}^{h/2} Q_{44} [g(z)]^2 dz \tag{20c}$$

Inserting Eq. (18) in Eq. (17), the following equation is found:

$$\begin{aligned} &A_{11} \frac{\partial^2 u_0}{\partial x^2} + A_{66} \frac{\partial^2 u_0}{\partial y^2} + (A_{12} + A_{66}) \frac{\partial^2 v}{\partial x \partial y} \\ &- B_{11} \frac{\partial^3 w_b}{\partial x^3} - (B_{12} + 2B_{66}) \frac{\partial^3 w_b}{\partial x \partial y^2} \\ &- B_{11}^s \frac{\partial^3 w_s}{\partial x^3} - (B_{12}^s + 2B_{66}^s) \frac{\partial^3 w_s}{\partial x \partial y^2} \\ &= (1 - \mu \nabla^2) \left[ I_0 \ddot{u}_0 - I_1 \frac{\partial \ddot{w}_b}{\partial x} - J_1 \frac{\partial \ddot{w}_s}{\partial x} \right], \end{aligned} \tag{21a}$$

$$\begin{aligned} &(A_{12} + A_{66}) \frac{\partial^2 u_0}{\partial x \partial y} + A_{66} \frac{\partial^2 v_0}{\partial x^2} + A_{22} \frac{\partial^2 v_0}{\partial y^2} \\ &- (B_{12} + 2B_{66}) \frac{\partial^3 w_b}{\partial x^2 \partial y} - B_{22} \frac{\partial^3 w_b}{\partial y^3} \\ &- B_{22}^s \frac{\partial^3 w_s}{\partial y^3} - (B_{12}^s + 2B_{66}^s) \frac{\partial^3 w_s}{\partial x^2 \partial y} \\ &= (1 - \mu \nabla^2) \left[ I_0 \ddot{v}_0 - I_1 \frac{\partial \ddot{w}_b}{\partial y} - J_1 \frac{\partial \ddot{w}_s}{\partial y} \right] \end{aligned} \tag{21b}$$

$$\begin{aligned}
 & B_{11} \frac{\partial^3 u_0}{\partial x^3} + (B_{12} + 2B_{66}) \frac{\partial^3 u_0}{\partial x \partial y^2} \\
 & + (B_{12} + 2B_{66}) \frac{\partial^3 v_0}{\partial x^2 \partial y} + B_{22} \frac{\partial^3 v_0}{\partial y^3} - D_{11} \frac{\partial^4 w_b}{\partial x^4} \\
 & - 2(D_{12} + 2D_{66}) \frac{\partial^4 w_b}{\partial x^2 \partial y^2} - D_{22} \frac{\partial^4 w_b}{\partial y^4} \\
 & - D_{11}^s \frac{\partial^4 w_s}{\partial x^4} - 2(D_{12}^s + 2D_{66}^s) \frac{\partial^4 w_s}{\partial x^2 \partial y^2} \\
 & - D_{22}^s \frac{\partial^4 w_s}{\partial y^4} = (1 - \mu \nabla^2) [I_0 (\ddot{w}_b + \ddot{w}_s) \\
 & + I_1 \left( \frac{\partial \ddot{u}_0}{\partial x} + \frac{\partial \ddot{v}_0}{\partial y} \right) - I_2 \nabla^2 \ddot{w}_b - J_2 \nabla^2 \ddot{w}_s]
 \end{aligned} \tag{21c}$$

$$\begin{aligned}
 & B_{11}^s \frac{\partial^3 u_0}{\partial x^3} + (B_{12}^s + 2B_{66}^s) \frac{\partial^3 u_0}{\partial x \partial y^2} \\
 & + (B_{12}^s + 2B_{66}^s) \frac{\partial^3 v_0}{\partial x^2 \partial y} + B_{22}^s \frac{\partial^3 v_0}{\partial y^3} - D_{11}^s \frac{\partial^4 w_b}{\partial x^4} \\
 & - 2(D_{12}^s + 2D_{66}^s) \frac{\partial^4 w_b}{\partial x^2 \partial y^2} - D_{22}^s \frac{\partial^4 w_b}{\partial y^4} \\
 & - H_{11}^s \frac{\partial^4 w_s}{\partial x^4} - 2(H_{12}^s + 2H_{66}^s) \frac{\partial^4 w_s}{\partial x^2 \partial y^2} \\
 & - H_{22}^s \frac{\partial^4 w_s}{\partial y^4} + A_{55}^s \frac{\partial^2 w_s}{\partial x^2} + A_{44}^s \frac{\partial^2 w_s}{\partial y^2} \\
 & = (1 - \mu \nabla^2) \left[ I_0 (\ddot{w}_b + \ddot{w}_s) + J_1 \left( \frac{\partial \ddot{u}_0}{\partial x} + \frac{\partial \ddot{v}_0}{\partial y} \right) \right. \\
 & \left. - J_2 \nabla^2 \ddot{w}_b - K_2 \nabla^2 \ddot{w}_s \right]
 \end{aligned} \tag{21d}$$

### 3 The solution of the problem

In the present part, solutions for the free vibration of FG nanoplate under four different boundary conditions are found.

The boundary conditions of a random edge are defined as follows:

Clamped (C) edge boundary conditions

$$u_0 = v_0 = w_b = w_s = \frac{\partial w_b}{\partial x} = \frac{\partial w_s}{\partial x} = 0 \text{ at } x = 0, a \tag{22a}$$

$$u_0 = v_0 = w_b = w_s = \frac{\partial w_b}{\partial y} = \frac{\partial w_s}{\partial y} = 0 \text{ at } y = 0, b \tag{22b}$$

Simply supported (S) edge boundary conditions

$$N_x = v_0 = w_b = w_s = M_x = 0 \text{ at } x = 0, a \tag{23a}$$

$$u_0 = N_y = w_b = w_s = M_y = 0 \text{ at } y = 0, b \tag{23b}$$

Free (F) edge boundary conditions

$$N_x = N_{xy} = \frac{\partial M_x}{\partial x} + 2 \frac{\partial M_{xy}}{\partial y} = Q_x = M_x = 0 \text{ at } x = 0, a \tag{24a}$$

$$N_{xy} = N_y + 2 \frac{\partial M_{xy}}{\partial y} + \frac{\partial M_y}{\partial y} = Q_y = M_y = 0 \text{ at } y = 0, b \tag{24b}$$

The subsequent appropriate expressions are utilized for the related boundary conditions

$$\begin{Bmatrix} u_0 \\ v_0 \\ w_b \\ w_s \end{Bmatrix} = \begin{Bmatrix} U_{mn} \frac{\partial X_m(x)}{\partial x} Y_n(y) e^{i\omega t} \\ V_{mn} X_m(x) \frac{\partial Y_n(y)}{\partial y} e^{i\omega t} \\ W_{bmn} X_m(x) Y_n(y) e^{i\omega t} \\ W_{smn} X_m(x) Y_n(y) e^{i\omega t} \end{Bmatrix} \tag{25}$$

where  $U_{mn}$ ,  $V_{mn}$ ,  $W_{bmn}$ , and  $W_{smn}$  identify the random parameters and  $\omega = \omega_{mn}$  shows the eigenfrequency related to  $(m, n)^{th}$  eigenmode.

The following functions for  $X_m(x)$  and  $Y_n(y)$  which are suggested by Reddy [54, 55] are utilized to satisfy various boundary conditions in Eqs. (22)–(24) and signify the deflected surface of the nanoplate approximately:

SSSS

$$\begin{aligned}
 X_m(x) &= \sin(\lambda x), \quad \lambda = \frac{m\pi}{a} \\
 Y_n(y) &= \sin(\beta y), \quad \beta = \frac{n\pi}{b}
 \end{aligned} \tag{26}$$

CCCC

$$\begin{aligned}
 X_m(x) &= [\sin(\lambda x) - \sinh(\lambda x)] - \left[ \frac{\sin(\lambda a) - \sinh(\lambda a)}{\cos(\lambda a) - \cosh(\lambda a)} \right] \\
 & [\cos(\lambda x) - \cosh(\lambda x)], \quad \lambda = \frac{(m + 0.5)\pi}{a} \\
 Y_n(y) &= [\sin(\beta y) - \sinh(\beta y)] - \left[ \frac{\sin(\beta b) - \sinh(\beta b)}{\cos(\beta b) - \cosh(\beta b)} \right] \\
 & [\cos(\beta y) - \cosh(\beta y)], \quad \beta = \frac{(n + 0.5)\pi}{b}
 \end{aligned} \tag{27}$$

CSCS

$$\begin{aligned}
 X_m(x) &= [\sin(\lambda x) - \sinh(\lambda x)] - \left[ \frac{\sin(\lambda a) + \sinh(\lambda a)}{\cos(\lambda a) + \cosh(\lambda a)} \right] \\
 &[\cos(\lambda x) - \cosh(\lambda x)], \lambda = \frac{(m + 0.25)\pi}{a} \\
 Y_n(y) &= [\sin(\beta y) - \sinh(\beta y)] - \left[ \frac{\sin(\beta b) + \sinh(\beta b)}{\cos(\beta b) + \cosh(\beta b)} \right] \\
 &[\cos(\beta y) - \cosh(\beta y)], \beta = \frac{(n + 0.25)\pi}{b}
 \end{aligned} \tag{28}$$

FCFC

$$\begin{aligned}
 X_m(x) &= [\sin(\lambda x) - \sinh(\lambda x)] - \left[ \frac{\sin(\lambda a) - \sinh(\lambda a)}{\cos(\lambda a) - \cosh(\lambda a)} \right] \\
 &[\cos(\lambda x) - \cosh(\lambda x)], \lambda = \frac{(m - 0.25)\pi}{a} \\
 Y_n(y) &= [\sin(\beta y) - \sinh(\beta y)] - \left[ \frac{\sin(\beta b) - \sinh(\beta b)}{\cos(\beta b) - \cosh(\beta b)} \right] \\
 &[\cos(\beta y) - \cosh(\beta y)], \beta = \frac{(n - 0.25)\pi}{b}
 \end{aligned} \tag{29}$$

Substituting the expression (25) in Eqs. (21) and multiplying each eigenfunction with the corresponding equation and integrating throughout the solution domain, and after some mathematical operations, the following equation is found

$$\begin{pmatrix} a_{11} & a_{12} & a_{13} & a_{14} \\ a_{21} & a_{22} & a_{23} & a_{24} \\ a_{31} & a_{32} & a_{33} & a_{34} \\ a_{41} & a_{42} & a_{43} & a_{44} \end{pmatrix} - \omega^2 \begin{pmatrix} m_{11} & 0 & m_{13} & m_{14} \\ 0 & m_{22} & m_{23} & m_{24} \\ m_{31} & m_{32} & m_{33} & m_{34} \\ m_{41} & m_{42} & m_{43} & m_{44} \end{pmatrix} \begin{pmatrix} U_{mn} \\ V_{mn} \\ W_{bmn} \\ W_{smn} \end{pmatrix} = \begin{pmatrix} 0 \\ 0 \\ 0 \\ 0 \end{pmatrix} \tag{30}$$

in which

$$\begin{aligned}
 a_{11} &= A_{11}\alpha_{12} + A_{66}\alpha_8, \quad a_{12} = (A_{12} + A_{66})\alpha_8, \\
 a_{13} &= -B_{11}\alpha_{12} - (B_{12} + 2B_{66})\alpha_8, \\
 a_{14} &= -(B_{12}^s + 2B_{66}^s)\alpha_8 - B_{11}^s\alpha_{12}, \\
 a_{21} &= (A_{12} + A_{66})\alpha_{10}, \quad a_{22} = A_{22}\alpha_4 + A_{66}\alpha_{10}, \\
 a_{23} &= -B_{22}\alpha_4 - (B_{12} + 2B_{66})\alpha_{10}, \\
 a_{24} &= -(B_{12}^s + 2B_{66}^s)\alpha_{10} - B_{22}^s\alpha_4, \\
 a_{31} &= B_{11}\alpha_{13} + (B_{12} + 2B_{66})\alpha_{11}, \\
 a_{32} &= (B_{12} + 2B_{66})\alpha_{11} + B_{22}\alpha_5, \\
 a_{33} &= -D_{11}\alpha_{13} - 2(D_{12} + 2D_{66})\alpha_{11} - D_{22}\alpha_5, \\
 a_{34} &= -D_{11}^s\alpha_{13} - 2(D_{12}^s + 2D_{66}^s)\alpha_{11} - D_{22}^s\alpha_5, \\
 a_{41} &= B_{11}^s\alpha_{13} + (B_{12}^s + 2B_{66}^s)\alpha_{11}, \\
 a_{42} &= (B_{12}^s + 2B_{66}^s)\alpha_{11} + B_{22}^s\alpha_5, \\
 a_{43} &= -D_{11}^s\alpha_{13} - 2(D_{12}^s + 2D_{66}^s)\alpha_{11} - D_{22}^s\alpha_5, \\
 a_{44} &= -H_{11}^s\alpha_{13} - 2(H_{12}^s + 2H_{66}^s)\alpha_{11} \\
 &\quad - H_{22}^s\alpha_5 + A_{44}^s\alpha_9 + A_{55}^s\alpha_3
 \end{aligned} \tag{31}$$

and

$$\begin{aligned}
 m_{11} &= -I_0[\alpha_6 - \mu(\alpha_{12} + \alpha_8)], \quad m_{12} = 0, \quad m_{13} = I_1[\alpha_6 - \mu(\alpha_{12} + \alpha_8)], \\
 m_{14} &= J_1[\alpha_6 - \mu(\alpha_{12} + \alpha_8)], \\
 m_{21} &= 0, \quad m_{22} = -I_0[\alpha_2 - \mu(\alpha_{10} + \alpha_4)], \\
 m_{23} &= I_1[\alpha_2 - \mu(\alpha_{10} + \alpha_4)], \quad m_{24} = J_1[\alpha_2 - \mu(\alpha_{10} + \alpha_4)], \\
 m_{31} &= -I_1[\alpha_9 - \mu(\alpha_{13} + \alpha_{11})], \quad m_{32} = -I_1[(\alpha_3 - \mu(\alpha_{11} + \alpha_5))], \\
 m_{33} &= -I_0[\alpha_1 - \mu(\alpha_9 + \alpha_3)] + I_2[(\alpha_9 + \alpha_3) - \mu(\alpha_{13} + \alpha_5 + 2\alpha_{11})], \\
 m_{34} &= -I_0[\alpha_1 - \mu(\alpha_9 + \alpha_3)] + J_2[(\alpha_9 + \alpha_3) - \mu(\alpha_{13} + \alpha_5 + 2\alpha_{11})], \\
 m_{41} &= -J_1[\alpha_9 - \mu(\alpha_{13} + \alpha_{11})], \quad m_{42} = -J_1[\alpha_3 - \mu(\alpha_{11} + \alpha_5)], \\
 m_{43} &= -I_0[\alpha_1 - \mu(\alpha_9 + \alpha_3)] + J_2[(\alpha_9 + \alpha_3) - \mu(\alpha_{13} + \alpha_5 + 2\alpha_{11})], \\
 m_{44} &= -I_0[\alpha_1 - \mu(\alpha_9 + \alpha_3)] + K_2[(\alpha_9 + \alpha_3) - \mu(\alpha_{13} + \alpha_5 + 2\alpha_{11})]
 \end{aligned} \tag{32}$$

with

**Table 1** The non-dimensional fundamental frequencies of FG nanoplate against the varying non-local parameter

Boundary conditions	Results	$\mu$ (nm <sup>2</sup> )								
		0			1			2		
		$k = 0$	$k = 1$	$k = 5$	$k = 0$	$k = 1$	$k = 5$	$k = 0$	$k = 1$	$k = 5$
SSSS	Present	0.0930	0.0547	0.0441	0.0850	0.0500	0.0403	0.0788	0.0463	0.0373
	Zargaripoor et al. [42]	0.0930	0.0504	0.0444	0.0850	0.0504	0.0405	0.0788	0.0467	0.0376
	Natarajan et al. [34]	-	-	0.0441	-	-	0.0403	-	-	0.0374
CCCC	Present	0.1618	0.0953	0.0764	0.1448	0.0853	0.0684	0.1322	0.0778	0.0625
	Zargaripoor et al. [42]	0.1597	0.0941	0.0753	0.1436	0.0846	0.0677	0.1315	0.0774	0.0677
	Natarajan et al. [34]	-	-	0.0758	-	-	0.0682	-	-	0.0624
SCSC	Present	0.1261	0.0742	0.0597	0.1136	0.0668	0.0538	0.1042	0.0613	0.0493
	Zargaripoor et al. [42]	0.1307	0.0771	0.0618	0.1185	0.0699	0.0560	0.1092	0.0644	0.0516

**Table 2** The non-dimensional frequencies of the first four modes of FG nanoplate with SSSS edges against the varying non-local parameter and power-law index

$k$	$\mu(\text{nm}^2)$	Results	$\Omega_1$	$\Omega_2$	$\Omega_3$	$\Omega_4$
0	0	Present	0.0930	0.2219	0.2219	0.3407
		Zargaripoor et al. [42]	0.0930	0.2225	0.2225	0.3407
	1	Present	0.0850	0.1816	0.1816	0.2547
		Zargaripoor et al. [42]	0.0850	0.1820	0.1820	0.2547
	2	Present	0.0788	0.1575	0.1575	0.2121
		Zargaripoor et al. [42]	0.0788	0.1578	0.1578	0.2122
1	0	Present	0.0547	0.1305	0.1305	0.2003
		Zargaripoor et al. [42]	0.0552	0.1310	0.1310	0.2008
	1	Present	0.0500	0.1068	0.1068	0.1497
		Zargaripoor et al. [42]	0.0504	0.1072	0.1072	0.1501
	2	Present	0.0463	0.0926	0.0926	0.1247
		Zargaripoor et al. [42]	0.0467	0.0930	0.0930	0.1250
5	0	Present	0.0441	0.1049	0.1049	0.1606
		Natarajan et al. [34]	0.0441	0.1051	0.1051	-
		Zargaripoor et al. [42]	0.0444	0.1052	0.1052	0.1608
	1	Present	0.0403	0.0858	0.0858	0.1201
		Natarajan et al. [34]	0.0403	0.0860	0.0860	-
	2	Zargaripoor et al. [42]	0.0405	0.0861	0.0861	0.1202
Present		0.0373	0.0744	0.0744	0.1000	
		Natarajan et al. [34]	0.0374	0.0745	0.0746	-
		Zargaripoor et al. [42]	0.0376	0.0747	0.0747	0.1002

**Table 3** The non-dimensional frequencies of the first four modes of FG nanoplate with CCCC edges against the varying non-local parameter and power-law index

$k$	$\mu(\text{nm}^2)$	Results	$\Omega_1$	$\Omega_2$	$\Omega_3$	$\Omega_4$
0	0	Present	0.1619	0.3147	0.3147	0.4454
		Zargaripoor et al. [42]	0.1597	0.3061	0.3061	0.4286
	1	Present	0.1448	0.2494	0.2494	0.3201
		Zargaripoor et al. [42]	0.1436	0.2450	0.2450	0.3129
	2	Present	0.1323	0.2129	0.2129	0.2628
		Zargaripoor et al. [42]	0.1315	0.2099	0.2099	0.2580
1	0	Present	0.0953	0.1853	0.1853	0.2621
		Zargaripoor et al. [42]	0.0941	0.1804	0.1804	0.2525
	1	Present	0.0853	0.1467	0.1467	0.1883
		Zargaripoor et al. [42]	0.0846	0.1443	0.1443	0.1842
	2	Present	0.0778	0.1252	0.1252	0.1545
		Zargaripoor et al. [42]	0.0774	0.1236	0.1236	0.1518
5	0	Present	0.0764	0.1482	0.1482	0.2092
		Natarajan et al. [34]	0.0758	0.1442	0.1455	-
		Zargaripoor et al. [42]	0.0753	0.1437	0.1437	0.2008
	1	Present	0.0684	0.1174	0.1174	0.1504
		Natarajan et al. [34]	0.0682	0.1157	0.1166	-
	2	Zargaripoor et al. [42]	0.0677	0.1151	0.1151	0.1467
Present		0.0625	0.1002	0.1002	0.1235	
		Natarajan et al. [34]	0.0624	0.0992	0.0999	-
		Zargaripoor et al. [42]	0.0620	0.0987	0.0987	0.1210



**Table 4** The change in the non-dimensional frequencies of the first four modes of FG square nanoplates under different boundary conditions against the varying non-local parameter and power-law index

<i>k</i>	$\mu(\text{nm}^2)$	SSSS				CCCC			
		$\Omega_1$	$\Omega_2$	$\Omega_3$	$\Omega_4$	$\Omega_1$	$\Omega_2$	$\Omega_3$	$\Omega_4$
0	0	0.0930	0.2219	0.2219	0.3407	0.1619	0.3147	0.3147	0.4454
	2	0.0788	0.1575	0.1575	0.2121	0.1323	0.2129	0.2129	0.2628
	4	0.0695	0.1287	0.1287	0.1671	0.1146	0.1714	0.1714	0.2045
2	0	0.0488	0.1162	0.1162	0.1782	0.0848	0.1646	0.1646	0.2327
	2	0.0413	0.0825	0.0825	0.1109	0.0693	0.1113	0.1113	0.1373
	4	0.0365	0.0674	0.0674	0.0874	0.0600	0.0896	0.0896	0.1068
4	0	0.0450	0.1071	0.1071	0.1640	0.0781	0.1513	0.1513	0.2137
	2	0.0381	0.0759	0.0759	0.1021	0.0638	0.1024	0.1024	0.1261
	4	0.0337	0.0621	0.0621	0.8043	0.0553	0.0824	0.0824	0.0981

<i>k</i>	$\mu(\text{nm}^2)$	CSCS				FCFC			
		$\Omega_1$	$\Omega_2$	$\Omega_3$	$\Omega_4$	$\Omega_1$	$\Omega_2$	$\Omega_3$	$\Omega_4$
0	0	0.1261	0.2681	0.2681	0.3920	0.1625	0.3152	0.3152	0.4453
	2	0.1042	0.1851	0.1851	0.2373	0.1325	0.2130	0.2130	0.2628
	4	0.0908	0.1500	0.1500	0.1857	0.1146	0.1715	0.1715	0.2045
2	0	0.0661	0.1403	0.1403	0.2049	0.0850	0.1647	0.1647	0.2324
	2	0.0546	0.0969	0.0969	0.1240	0.0694	0.1113	0.1113	0.1372
	4	0.0476	0.0785	0.0785	0.0971	0.0600	0.0896	0.0896	0.1068
4	0	0.0609	0.1292	0.1292	0.1884	0.0783	0.1514	0.1514	0.2135
	2	0.0504	0.0892	0.0892	0.1141	0.0639	0.1024	0.1024	0.1261
	4	0.0439	0.0723	0.0723	0.0893	0.0553	0.0824	0.0824	0.0981

**Table 5** The change in the non-dimensional fundamental frequency of FG rectangular nanoplates under different boundary conditions against the varying non-local parameter and power-law index

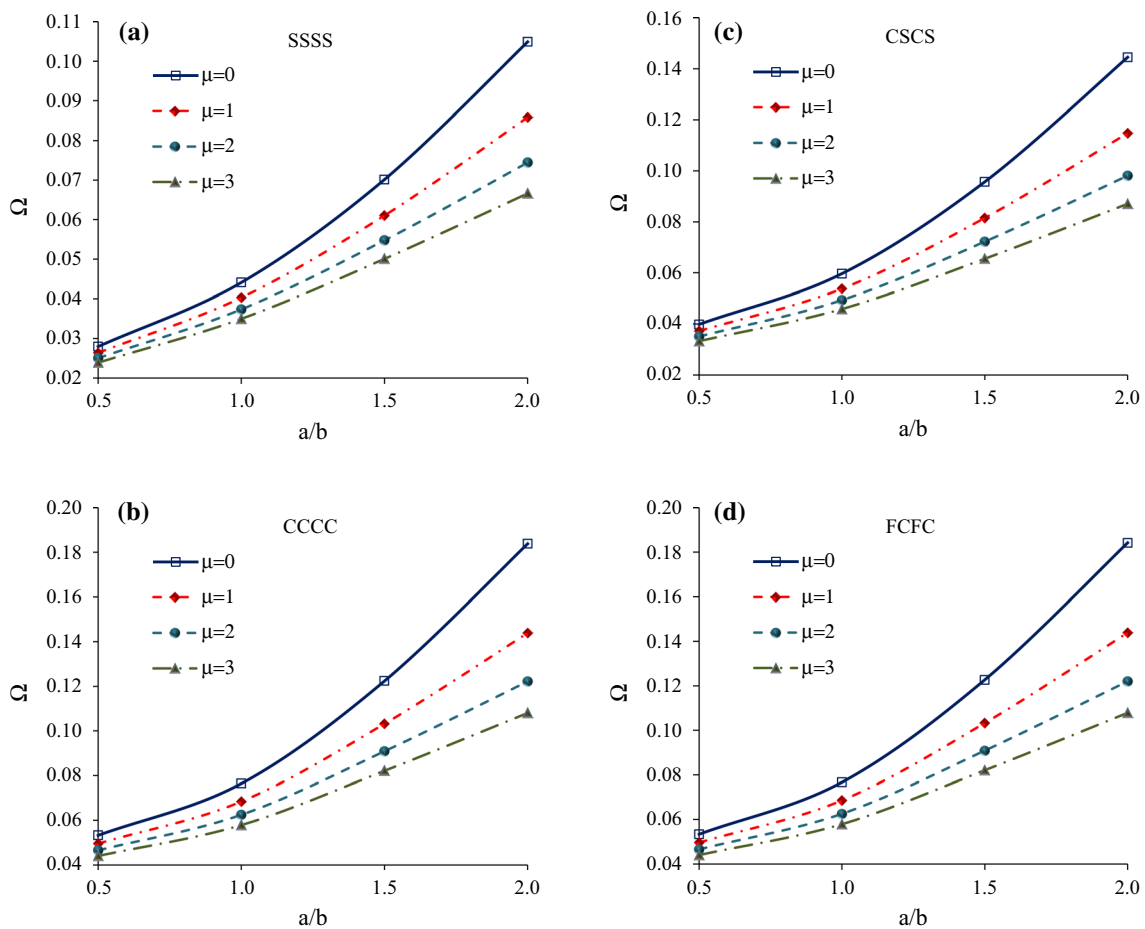
<i>k</i>	$\mu(\text{nm}^2)$	$\Omega_1$			
		SSSS	CCCC	CSCS	FCFC
5	0	0.1049	0.1445	0.1838	0.1842
	1	0.0859	0.1148	0.1439	0.1439
	2	0.0744	0.0981	0.1222	0.1220
	3	0.0666	0.0871	0.1080	0.1078
	4	0.0608	0.0791	0.0979	0.0977
	5	0.0563	0.0729	0.0901	0.0899

<i>k</i>	$\mu(\text{nm}^2)$	$\Omega_1$			
		SSSS	CCCC	CSCS	FCFC
0	1	0.1816	0.2437	0.3069	0.3072
1		0.1068	0.1434	0.1808	0.1806
2		0.0951	0.1275	0.1603	0.1602
3		0.0904	0.1209	0.1518	0.1517
4		0.0876	0.1172	0.1470	0.1469
5		0.0859	0.1148	0.1439	0.1439

**Table 6** The change in the frequency ratio of FG rectangular nanoplates under different boundary conditions against the non-local parameter

$\mu$ (nm <sup>2</sup> )	SSSS				CCCC			
	$F_{r1}$	$F_{r2}$	$F_{r3}$	$F_{r4}$	$F_{r1}$	$F_{r2}$	$F_{r3}$	$F_{r4}$
0	1	1	1	1	1	1	1	1
1	0.8183	0.6111	0.7475	0.5799	0.7820	0.5743	0.7111	0.5447
2	0.7094	0.4792	0.6227	0.4496	0.6636	0.4444	0.5816	0.4173
3	0.6349	0.4071	0.5448	0.3801	0.5866	0.3754	0.5042	0.3511
4	0.5799	0.3601	0.4904	0.3353	0.5314	0.3309	0.4512	0.3088
5	0.5370	0.3264	0.4496	0.3033	0.4893	0.2993	0.4120	0.2789
$\mu$ (nm <sup>2</sup> )	CSCS				FCFC			
	$F_{r1}$	$F_{r2}$	$F_{r3}$	$F_{r4}$	$F_{r1}$	$F_{r2}$	$F_{r3}$	$F_{r4}$
0	1	1	1	1	1	1	1	1
1	0.7941	0.5908	0.7252	0.5609	0.7805	0.5753	0.7103	0.5458
2	0.6786	0.4598	0.5974	0.4321	0.6618	0.4453	0.5809	0.4183
3	0.6022	0.3894	0.5196	0.3643	0.5847	0.3762	0.5034	0.3519
4	0.5469	0.3438	0.4660	0.3209	0.5295	0.3318	0.4505	0.3096
5	0.5045	0.3112	0.4262	0.2899	0.4875	0.3000	0.4114	0.2796



**Fig. 2** The change in the non-dimensional fundamental frequencies of FG rectangular nanoplates under different boundary conditions against the varying aspect ratio

$$\begin{aligned}
 (\alpha_1, \alpha_3, \alpha_5) &= \int_0^b \int_0^a (X_m Y_n, X_m Y_n'', X_m Y_n''') X_m Y_n dx dy \\
 (\alpha_2, \alpha_4, \alpha_{10}) &= \int_0^b \int_0^a (X_m Y_n', X_m Y_n'', X_m Y_n''') X_m Y_n' dx dy \\
 (\alpha_6, \alpha_8, \alpha_{12}) &= \int_0^b \int_0^a (X_m' Y_n, X_m'' Y_n, X_m''' Y_n) X_m' Y_n dx dy \\
 (\alpha_7, \alpha_9, \alpha_{11}, \alpha_{13}) &= \int_0^b \int_0^a (X_m' Y_n', X_m'' Y_n, X_m''' Y_n, X_m'''' Y_n) X_m' Y_n dx dy
 \end{aligned} \quad (33)$$

The nontrivial solution of the present problem is found equating the determinant of Eq. (30) to zero.

## 4 The numerical results and discussion

Herein numerous examples are given for validating the accuracy of the current solution procedure as well as the investigation of the natural frequencies of FG nanoplate considering four different cases of boundary conditions. For this aim, in Tables 1, 2 and 3 comparison studies are given to validate the accuracy of the present work. Then, detailed analyses are performed to study the influence of different parameters such as vibration mode, the aspect ratio, boundary conditions, power-law index, and non-local parameter on natural frequencies of the FG nanoplate in Tables 4, 5 and 6 and Fig. 2.

In all numerical analyses, the free vibration analysis is performed considering that the top surface of the plate is  $\text{Si}_3\text{N}_4$  (ceramic) and the bottom surface is SUS304 (metal). Young's modulus,  $E$ , and mass density,  $\rho$ , are taken to be  $E_c = 348.43$  GPa,  $\rho_c = 2370$  kg/m<sup>3</sup> for  $\text{Si}_3\text{N}_4$  and  $E_m = 201.01$  GPa,  $\rho_m = 8166$  kg/m<sup>3</sup> for SUS304. Besides, the non-dimensional natural frequency,  $\Omega$ , and frequency ratio,  $F_r$ , are expressed as follows:

$$\Omega_i = \omega_i h \sqrt{\frac{\rho_c}{G_c}}, \quad F_{r_i} = \frac{\bar{\omega}_{i_{NL}}}{\bar{\omega}_{i_L}}, \quad i = 1, 2, 3, 4$$

where  $\rho_c$  and  $G_c$  are the mass density and shear modulus of the ceramic constituent, respectively,  $\bar{\omega}_{i_{NL}}$  and  $\bar{\omega}_{i_L}$  are the non-local and local ( $\mu = 0$ ) non-dimensional frequencies, respectively.

### 4.1 Comparison examples

**Example 1** The non-dimensional fundamental natural frequencies,  $\Omega_1$ , of FG square nanoplates versus the varying non-local parameter ( $\mu$ ) are checked against the findings of

Natarajan et al. [34] and Zargaripour et al. [42], in Table 1. Here, fully simply supported (SSSS), fully clamped (CCCC) and SCSC edge conditions,  $a/b = 1$  and  $a/h = 10$ , are considered.

**Example 2** The non-dimensional frequencies,  $\Omega_i$ , of the first four modes of FG square nanoplates versus varying non-local parameter ( $\mu$ ) and power-law exponent ( $k$ ) are checked against the findings of Natarajan et al. [34] and Zargaripour et al. [42], in Table 2. Here, SSSS edge conditions  $a/b = 1$  and  $a/h = 10$  are considered.

**Example 3** The non-dimensional frequencies,  $\Omega_i$ , of the first four modes of FG square nanoplates versus varying non-local parameter ( $\mu$ ) and power-law exponent ( $k$ ) are checked against the findings of Natarajan et al. [34] and Zargaripour et al. [42], in Table 2. Here, CCCC edge conditions  $a/b = 1$  and  $a/h = 10$  are considered.

Consequently, it is realized that the obtained results are coinciding with the existing ones.

### 4.2 Illustrative examples

**Example 4** The influence of varying non-local parameter,  $\mu$ , and power-law index,  $k$ , on non-dimensional first four natural frequencies,  $\Omega_i$  ( $i = 1, 2, 3, 4$ ), of FG nanoplates under different boundary conditions is examined for square and rectangular plates in Tables 5 and 6, respectively. Here,  $a/h = 10$ ,  $a/b = 1$ , and  $a/b = 2$  are considered. The findings revealed that the values of  $\Omega_i$  decrease with the increment of  $k$  since the percentage of metal phases that are weaker than ceramic phases become more prominent. The influence of the variation of  $k$  on the values of  $\Omega_i$  is independent of the variation of the non-local parameter, mode number, and edge conditions. Furthermore, the values of  $\Omega_i$  decrease with the increase in the  $\mu$ . Note that the influence of the variation of  $\mu$  on the values of  $\Omega_i$  is changing according to the boundary conditions, as well as the influence of the variation of  $\mu$  on the values of  $\Omega_i$  increases with the increment of the number of the mode, while it is independent of the variation of the  $k$ .

**Example 5** The influence of varying non-local parameter,  $\mu$ , on the frequency ratio,  $F_{r_i}$  ( $i = 1, 2, 3, 4$ ), of FG rectangular nanoplates versus four distinct boundary conditions is examined in Table 6. Here,  $k = 2$ ,  $a/h = 10$ , and  $a/b = 2$  are considered. The results revealed that the values of  $F_{r_i}$  decrease with the increment of  $\mu$ . Note that the influence of the variation of  $\mu$  on the values of  $F_{r_i}$  which is changing according to the boundary conditions, as well as the influence of the variation of  $\mu$  on the values of  $F_{r_i}$  frequency ratio of FG nanoplates changes with the number of the mode.

**Example 6** The influence of varying aspect ratio,  $a/b$  and non-local parameter,  $\mu$  ( $\text{nm}^2$ ), on the non-dimensional fundamental frequencies,  $\Omega_1$ , of FG rectangular nanoplates versus four distinct boundary conditions is examined in Fig. 2. Here,  $k = 5$ ,  $a/h = 10$  are considered. The results indicated that the values of  $\Omega_1$  increase with the increase in  $a/b$ . Note that the influence of the variation of  $a/b$  on the values of  $\Omega_1$  is changing according to the boundary conditions, as well as the influence of the variation of  $a/b$  on the values of  $\Omega_1$  decreases with the increment of  $\mu$ .

## 5 Conclusions

In the present study, an analytical solution for the free vibration of nanoplates made of FGMs under four different boundary conditions was provided. For this aim, a new refined plate theory with four variables based on the theory of non-local elasticity including the small-scale influence. Here, the number of unknowns and governing equations of the present model were reduced to four separating the vertical displacement into shear and bending components, and so the number of unknowns has become less than the other alternative theories. The influence of the different parameters such as vibration mode, the aspect ratio, boundary conditions, power-law index, and non-local parameter on the natural frequencies of the FG nanoplate is discussed, in detail.

In sum, the following results were obtained:

- The non-dimensional natural frequencies reduce with the increment of the power-law index
- The non-dimensional natural frequencies reduce with the increment of the non-local parameter
- The influence of variation of the non-local parameter on non-dimensional natural frequencies increases with the increment of the mode number
- The frequency ratio reduces with the increment of non-local parameter
- The influence of non-local parameter on the frequency ratio changes with mode number
- The values of non-dimensional fundamental natural frequency increase with the increase in aspect ratio.
- The influence of aspect ratio on the non-dimensional fundamental natural frequency decreases with the increment of the non-local parameter
- All said influence on non-dimensional natural frequencies changes depending on boundary conditions

Consequently, it is decided that considered factors have key influences on the natural frequencies of FG nanoplates. Furthermore, the proposed exact solution method not only satisfactorily handled the present problem and yielded

successful results but also it supplied ease for the non-local vibration analysis of FG nanoplates. In the future studies, the presented solution procedure will be extended for mechanical behaviors of other types of structures composed of varied materials with macro-/micro-dimensions.

## References

1. Koizumi M (1993) The concept of FGM. *Ceram Trans Funct Graded Mater* 34:3–10
2. Koizumi M (1997) FGM activities in Japan. *Compos Part B Eng* 28:1–4. [https://doi.org/10.1016/S1359-8368\(96\)00016-9](https://doi.org/10.1016/S1359-8368(96)00016-9)
3. Bellifa H, Benrahou KH, Hadji L et al (2016) Bending and free vibration analysis of functionally graded plates using a simple shear deformation theory and the concept the neutral surface position. *J Braz Soc Mech Sci Eng* 38:265–275. <https://doi.org/10.1007/s40430-015-0354-0>
4. Karami B, Janghorban M, Tounsi A (2019) On pre-stressed functionally graded anisotropic nanoshell in magnetic field. *J Braz Soc Mech Sci Eng* 41:495. <https://doi.org/10.1007/s40430-019-1996-0>
5. Žur KK (2019) Free-vibration analysis of discrete-continuous functionally graded circular plate via the Neumann series method. *Appl Math Model* 73:166–189. <https://doi.org/10.1016/j.apm.2019.02.047>
6. AlSaid-Alwan HHS, Avcar M (2020) Analytical solution of free vibration of FG beam utilizing different types of beam theories: a comparative study. *Comput Concr* 26:285–292. <https://doi.org/10.12989/cac.2020.26.3.285>
7. Chikr SC, Kaci A, Bousahla AA et al (2020) A novel four-unknown integral model for buckling response of FG sandwich plates resting on elastic foundations under various boundary conditions using Galerkin's approach. *Geomech Eng* 21:471. <https://doi.org/10.12989/GAE.2020.21.5.471>
8. Hadji L, Avcar M (2020) Free vibration analysis of FG porous sandwich plates under various boundary conditions. *J Appl Comput Mech*. <https://doi.org/10.22055/JACM.2020.35328.2628>
9. Rezaiee-Pajand M, Arabi E, Moradi AH (2021) Static and dynamic analysis of FG plates using a locking free 3D plate bending element. *J Braz Soc Mech Sci Eng* 43:18. <https://doi.org/10.1007/s40430-020-02744-1>
10. Tati A (2021) A five unknowns high order shear deformation finite element model for functionally graded plates bending behavior analysis. *J Braz Soc Mech Sci Eng* 43:45. <https://doi.org/10.1007/s40430-020-02736-1>
11. Iijima S (1991) Helical microtubules of graphitic carbon. *Nature*. <https://doi.org/10.1038/354056a0>
12. Reddy JN, Pang SD (2008) Nonlocal continuum theories of beams for the analysis of carbon nanotubes. *J Appl Phys* 103:023511. <https://doi.org/10.1063/1.2833431>
13. Kiani K (2014) Axial buckling analysis of vertically aligned ensembles of single-walled carbon nanotubes using nonlocal discrete and continuous models. *Acta Mech* 225:3569–3589. <https://doi.org/10.1007/s00707-014-1107-3>
14. Akgöz B, Civalek Ö (2015) A microstructure-dependent sinusoidal plate model based on the strain gradient elasticity theory. *Acta Mech* 226:2277–2294. <https://doi.org/10.1007/s00707-015-1308-4>
15. Karličić D, Murmu T, Adhikari S, McCarthy M (2015) Non-local structural mechanics. Wiley, Hoboken
16. Kiani K, Soltani S (2018) Three-dimensional dynamics of beam-like nanorotors on the basis of newly developed nonlocal shear deformable mode shapes. *Eur Phys J Plus* 133:1–21. <https://doi.org/10.1140/epjp/i2018-12197-4>

17. Jalaei MH, Civalek O (2019) On dynamic instability of magnetically embedded viscoelastic porous FG nanobeam. *Int J Eng Sci* 143:14–32. <https://doi.org/10.1016/j.ijengsci.2019.06.013>
18. Kiani K, Soltani S (2020) Nonlocal longitudinal, flapwise, and chordwise vibrations of rotary doubly coaxial/non-coaxial nanobeams as nanomotors. *Int J Mech Sci* 168:105291. <https://doi.org/10.1016/j.ijmechsci.2019.105291>
19. Civalek Ö, Dastjerdi S, Akbaş ŞD, Akgöz B (2021) Vibration analysis of carbon nanotube-reinforced composite microbeams. *Math Methods Appl Sci* 44:7069. <https://doi.org/10.1002/mma.7069>
20. Farahmand H (2021) A variational approach for analytical buckling solution of moderately thick microplate using strain gradient theory incorporating two-variable refined plate theory: a benchmark study. *J Braz Soc Mech Sci Eng*. <https://doi.org/10.1007/s40430-020-02766-9>
21. Hadji LM (2021) Nonlocal free vibration analysis of porous FG nanobeams using hyperbolic shear deformation beam theory. *Adv Nano Res* 10:281–293. <https://doi.org/10.12989/ANR.2021.10.3.281>
22. Eringen AC (1972) Linear theory of nonlocal elasticity and dispersion of plane waves. *Int J Eng Sci* 10:425–435. [https://doi.org/10.1016/0020-7225\(72\)90050-X](https://doi.org/10.1016/0020-7225(72)90050-X)
23. Eringen AC (1983) On differential equations of nonlocal elasticity and solutions of screw dislocation and surface waves. *J Appl Phys* 54:4703–4710. <https://doi.org/10.1063/1.332803>
24. Thai HT, Vo TP, Nguyen TK, Kim SE (2017) A review of continuum mechanics models for size-dependent analysis of beams and plates. *Compos Struct* 177:196–219
25. Fu Y, Du H, Zhang S (2003) Functionally graded TiN/TiNi shape memory alloy films. *Mater Lett* 57:2995–2999. [https://doi.org/10.1016/S0167-577X\(02\)01419-2](https://doi.org/10.1016/S0167-577X(02)01419-2)
26. Lü CF, Lim CW, Chen WQ (2009) Size-dependent elastic behavior of FGM ultra-thin films based on generalized refined theory. *Int J Solids Struct* 46:1176–1185. <https://doi.org/10.1016/j.ijsolstr.2008.10.012>
27. Hasanyan DJ, Batra RC, Harutyunyan S (2008) Pull-in instabilities in functionally graded microthermoelectromechanical systems. *J Therm Stress* 31:1006–1021. <https://doi.org/10.1080/01495730802250714>
28. Zhang J, Fu Y (2012) Pull-in analysis of electrically actuated viscoelastic microbeams based on a modified couple stress theory. *Meccanica* 47:1649–1658. <https://doi.org/10.1007/s11012-012-9545-2>
29. Rahaeifard M, Kahrobaiyan MH, Ahmadian MT (2009) Sensitivity analysis of atomic force microscope cantilever made of functionally graded materials. In: *Proceedings of the ASME design engineering technical conference*. American Society of Mechanical Engineers Digital Collection, pp 539–544
30. Kiani K (2011) Nonlocal continuum-based modeling of a nanoplate subjected to a moving nanoparticle. Part I: theoretical formulations. *Phys E Low-Dimensional Syst Nanostruct* 44:229–248. <https://doi.org/10.1016/j.physe.2011.08.020>
31. Kiani K (2011) Nonlocal continuum-based modeling of a nanoplate subjected to a moving nanoparticle. Part II: parametric studies. *Phys E Low-Dimensional Syst Nanostruct* 44:249–269. <https://doi.org/10.1016/j.physe.2011.08.021>
32. Kiani K (2013) Vibrations of biaxially tensioned-embedded nanoplates for nanoparticle delivery. *Indian J Sci Technol* 6:4894–4902. <https://doi.org/10.17485/ijst/2013/v6i7.16>
33. Gürses M, Akgöz B, Civalek Ö (2012) Mathematical modeling of vibration problem of nano-sized annular sector plates using the nonlocal continuum theory via eight-node discrete singular convolution transformation. *Appl Math Comput* 219:3226–3240. <https://doi.org/10.1016/j.amc.2012.09.062>
34. Natarajan S, Chakraborty S, Thangavel M et al (2012) Size-dependent free flexural vibration behavior of functionally graded nanoplates. *Comput Mater Sci* 65:74–80. <https://doi.org/10.1016/j.commatsci.2012.06.031>
35. Ansari R, Faghieh Shojaei M, Shahabodini A, Bazdid-Vahdati M (2015) Three-dimensional bending and vibration analysis of functionally graded nanoplates by a novel differential quadrature-based approach. *Compos Struct* 131:753–764. <https://doi.org/10.1016/j.compstruct.2015.06.027>
36. Daneshmehr A, Rajabpoor A, Hadi A (2015) Size dependent free vibration analysis of nanoplates made of functionally graded materials based on nonlocal elasticity theory with high order theories. *Int J Eng Sci* 95:23–35. <https://doi.org/10.1016/j.ijengsci.2015.05.011>
37. Nami MR, Janghorban M (2015) Free vibration analysis of rectangular nanoplates based on two-variable refined plate theory using a new strain gradient elasticity theory. *J Braz Soc Mech Sci Eng* 37:313–324. <https://doi.org/10.1007/s40430-014-0169-4>
38. Mechab I, Mechab B, Benaissa S et al (2016) Free vibration analysis of FGM nanoplate with porosities resting on Winkler Pasternak elastic foundations based on two-variable refined plate theories. *J Braz Soc Mech Sci Eng* 38:2193–2211. <https://doi.org/10.1007/s40430-015-0482-6>
39. Phung-Van P, Thai CH, Ferreira AJM, Rabczuk T (2020) Isogeometric nonlinear transient analysis of porous FGM plates subjected to hydro-thermo-mechanical loads. *Thin-Walled Struct* 148:106497. <https://doi.org/10.1016/j.tws.2019.106497>
40. Arefi M, Mohammad-Rezaei Bidgoli E, Dimitri R, Tornabene F (2018) Free vibrations of functionally graded polymer composite nanoplates reinforced with graphene nanoplatelets. *Aerosp Sci Technol* 81:108–117. <https://doi.org/10.1016/j.ast.2018.07.036>
41. Barati MR, Shahverdi H (2018) Nonlinear thermal vibration analysis of refined shear deformable FG nanoplates: two semi-analytical solutions. *J Braz Soc Mech Sci Eng* 40:1–15. <https://doi.org/10.1007/s40430-018-0968-0>
42. Zargaripoor A, Daneshmehr A, Isaac Hosseini I, Rajabpoor A (2018) Free vibration analysis of nanoplates made of functionally graded materials based on nonlocal elasticity theory using finite element method. *J Comput Appl Mech* 49:86–101. <https://doi.org/10.22059/jcamech.2018.248906.223>
43. Barretta R, Faghidian SA, Marotti de Sciarra F (2019) Stress-driven nonlocal integral elasticity for axisymmetric nano-plates. *Int J Eng Sci* 136:38–52. <https://doi.org/10.1016/j.ijengsci.2019.01.003>
44. Ruocco E, Mallardo V (2019) Buckling and vibration analysis nanoplates with imperfections. *Appl Math Comput* 357:282–296. <https://doi.org/10.1016/j.amc.2019.03.030>
45. Sharifi Z, Khordad R, Gharaati A, Forozani G (2019) An analytical study of vibration in functionally graded piezoelectric nanoplates: nonlocal strain gradient theory. *Appl Math Mech (English Ed)* 40:1723–1740. <https://doi.org/10.1007/s10483-019-2545-8>
46. Daikh AA, Draï A, Bensaïd I et al (2020) On vibration of functionally graded sandwich nanoplates in the thermal environment. *J Sandw Struct Mater*. <https://doi.org/10.1177/1099636220909790>
47. Tran VK, Pham QH, Nguyen-Thoi T (2020) A finite element formulation using four-unknown incorporating nonlocal theory for bending and free vibration analysis of functionally graded nanoplates resting on elastic medium foundations. *Eng Comput* 1:3. <https://doi.org/10.1007/s00366-020-01107-7>
48. Zenkour AM, Hafed ZS, Radwan AF (2020) Bending analysis of functionally graded nanoscale plates by using nonlocal mixed variational formula. *Mathematics* 8:1162. <https://doi.org/10.3390/math8071162>
49. Liu C, Ke LL, Wang YS et al (2013) Thermo-electro-mechanical vibration of piezoelectric nanoplates based on the nonlocal theory.

- Compos Struct 106:167–174. <https://doi.org/10.1016/j.composit.2013.05.031>
50. Malekzadeh P, Shojaee M (2013) Free vibration of nanoplates based on a nonlocal two-variable refined plate theory. *Compos Struct* 95:443–452. <https://doi.org/10.1016/j.compstruct.2012.07.006>
  51. Kiani K (2014) Free vibration of conducting nanoplates exposed to unidirectional in-plane magnetic fields using nonlocal shear deformable plate theories. *Phys E Low-Dimensional Syst Nanostruct* 57:179–192. <https://doi.org/10.1016/j.physe.2013.10.034>
  52. Meksi R, Benyoucef S, Mahmoudi A et al (2019) An analytical solution for bending, buckling and vibration responses of FGM sandwich plates. *J Sandw Struct Mater* 21:727–757. <https://doi.org/10.1177/1099636217698443>
  53. Zaoui FZ, Ouinas D, Tounsi A (2019) New 2D and quasi-3D shear deformation theories for free vibration of functionally graded plates on elastic foundations. *Compos Part B Eng* 159:231–247. <https://doi.org/10.1016/j.compositesb.2018.09.051>
  54. Reddy JN (1997) *Mechanics of composite materials and structures: theory and analysis*. CRC Press, Boca Raton
  55. Reddy JN (2004) *Mechanics of laminated composite plates and shells: theory and analysis*, 2nd edn. CRC Press, Boca Raton

**Publisher's Note** Springer Nature remains neutral with regard to jurisdictional claims in published maps and institutional affiliations.